Targeting Caspase-12 to Preserve Vision in Mice With Inherited Retinal Degeneration

Yogesh Bhootada,[1] Shreyasi Choudhury,[2] Clark Gully,[1] and Marina Gorbatyuk[1]

[1]Department of Vision Sciences, University of Alabama at Birmingham, Birmingham, Alabama, United States
[2]Department of Cell Biology and Anatomy, University of North Texas Health Science Center, North Texas Eye Research Institute, Fort Worth, Texas, United States

Correspondence: Marina Gorbatyuk, Department of Vision Sciences, University of Alabama at Birmingham, 1670 University Boulevard, Birmingham, AL 35233, USA; mgortk@uab.edu.

Submitted: March 20, 2015
Accepted: June 15, 2015

Citation: Bhootada Y, Choudhury S, Gully C, Gorbatyuk M. Targeting caspase-12 to preserve vision in mice with inherited retinal degeneration. *Invest Ophthalmol Vis Sci*. 2015;56:4725–4733. DOI:10.1167/iovs.15-16924

Purpose. The unfolded protein response is known to contribute to the inherited retinal pathology observed in T17M rhodopsin (T17M) mice. Recently it has been demonstrated that the endoplasmic reticulum stress–associated caspase-12 is activated during progression of retinal degeneration in different animal models. Therefore, we wanted to explore the role of caspase-12 in the mechanism of retinopathy in T17M mice and determine if inhibiting apoptosis in this way is a viable approach for halting retinal degeneration.

Methods. One, two-, and three-month-old C57BL6/J, caspase-12$^{-/-}$, T17M, and T17M caspase-12$^{-/-}$ mice were analyzed by scotopic ERG, spectral-domain optical coherence tomography (SD-OCT), histology, quantitative (q)RT-PCR, and Western blot of retinal RNA and protein extracts. Calpain and caspase-3/7 activity assays were measured in postnatal (P) day 30 retinal extracts.

Results. Caspase-12 ablation significantly prevented a decline in the a- and b-wave ERG amplitudes in T17M mice during three months, increasing the amplitudes from 232% to 212% and from 160% to 138%, respectively, as compared to T17M retinas. The SD-OCT results and photoreceptor row counts demonstrated preservation of retinal structural integrity and postponed photoreceptor cell death. The delay in photoreceptor cell death was due to significant decreases in the activity of caspase-3/7 and calpain, which correlated with an increase in calpastatin expression.

Conclusions. We validated caspase-12 as a therapeutic target, ablation of which significantly protects T17M photoreceptors from deterioration. Although the inhibition of apoptotic activity alone was not sufficient to rescue T17M photoreceptors, in combination with other nonapoptotic targets, caspase-12 could be used to treat inherited retinopathy.

Keywords: retinal degeneration, unfolded protein response, caspase-12

Mice expressing a mutant form of human rhodopsin with a threonine to methionine substitution at position 17 (T17M) develop severe retinal degeneration and thus mimic the human autosomal dominant retinitis pigmentosa (ADRP).[1,2] The study of molecular mechanisms underlying the retinopathy in these mice has demonstrated that the unfolded protein response (UPR), along with inflammatory signaling, significantly contributes to the progression of retinal degeneration.[3] Thus, the activation of all three UPR branches, including protein kinase R–like endoplasmic reticulum kinase (PERK), activating transcriptional factor 6 (ATF6), and inositol-requiring enzyme 1 (IRE1), has been detected in T17M retinas as early as postnatal (P) day 15. Moreover, we have recently revealed that the rate of retinal degeneration could be significantly altered in these mice by modifying the expression of UPR hallmark proteins. For example, we found that full knockout of the UPR proapoptotic CHOP protein in degenerating retinas dramatically accelerated the rate of retinal degeneration[4,5] while full ablation of the UPR downstream marker, the endoplasmic reticulum (ER) stress–associated caspase (Csp)-7, significantly slowed the rate of retinal degeneration.[6]

In addition to Csp-7, Csp-12 localizes to the Golgi complex and is also activated during ER stress.[7] Several studies have suggested that Csp-12 acts as an initiator Csp during ER stress–induced apoptosis, activating an effector Csp-3 or -7, which then cleaves key substrates required for normal cellular functions, thus leading to apoptosis.[8] Recently, it has also been reported that Csp-12–deficient mice are resistant to ER stress–induced apoptosis, but their cells do undergo apoptosis in response to other stimuli. Thus, in experiments with primary cortical neurons, the link between ER stress and Csp-12 activation has been proposed through demonstration of the reduced susceptibility of Csp-12$^{-/-}$ neurons to Aβ-induced UPR activation and subsequent cell death.[9] These experiments have clearly demonstrated that activation of Csp-12 during ER stress plays a proapoptotic role and contributes to neuronal death in Alzheimer's disease.[9]

Recent studies have proposed that there are two mechanisms for ER stress–mediated Csp-12 activation that act in different compartments of the cell. The first involves the interaction of proCsp-12 with the IRE1–TRAF2 complex (IRE1 UPR arm) on the cytosolic side of the ER membrane.[10] This interaction occurs as a result of altered complex formation between IRE1α and TRAF2 (tumor necrosis factor receptor-associated factor 2) in response to ER stress and modified activity of Jun N-terminal inhibitory kinase (JIK) against its

binding partner IRE1a.[10] This suggests that Csp-12 activated by TRAF2 plays a crucial role in signal transduction from IRE1 to downstream signaling molecules and thus links the stress sensor molecule IRE1 to the activation of Csp-12. The second mechanism for Csp-12 activation occurs in the cytosol, where an increase in Ca^{2+} concentration results in calpain activation. The μ-calpain activation in turn precedes expression/activation of Csp-12 and is required for activation/cleavage of Csp-12.[11] Given that a cytosolic Ca^{2+} increase could also occur in response to ER stress, this pathway along with the above-mentioned TRAF2-pathway points to Csp-12 as the ER stress–induced Csp promoting apoptosis.

Involvement of Csp-12 in the mechanisms of several different retinopathies has been recently described in a number of studies.[12–16] Although a combination of inhibiting Csp-12, upregulating the ER-resident chaperone BiP, and inhibiting CAP-dependent translation, has been proposed as the most efficient way to maintain BBS-12 photoreceptors,[13] the direct impact of inhibiting Csp-12 on loss of photoreceptor function and cell death has yet to be shown, since Csp-12 has not been previously assigned a direct role in retinal degeneration. The Csp-12 inhibitor INH (the synthetic peptide Z-Ala-Thr-Ala-Asp(O-methyl)-fluoromethyl-ketone) in this study has been used in combination with other drugs such as guanabenz and valproic acid, pointing to the necessity of conducting a study demonstrating a direct link between Csp-12 activation and retinal degeneration.

Therefore, in the current study we explored the role of Csp-12 in the mechanism of retinal pathogenesis in T17M mice. Our goal was to determine if ER stress–induced apoptosis played a role in ADRP photoreceptor demise and whether the therapeutic approach of targeting ER stress–promoted apoptosis was sufficient to rescue ADRP photoreceptors. Building on a previous study that looked exclusively at Csp-7 in T17M mice, the current work genetically modulated Csp-12 activity in T17M mice and compared the results to our previous findings. We also attempted to answer the question whether blocking apoptosis overall proved sufficient to rescue ADRP retinas and prevent further loss of retinal integrity. Our data point to inhibition of Csp-12 as a potential therapeutic approach that significantly slows retinal degeneration and together with other nonapoptotic targets could dramatically delay photoreceptor cell death.

Materials and Methods

Animals

All animal groups were maintained on a C57BL6/J (wild-type [wt]) background. The Csp-12$^{-/-}$ mice were created as previously described.[17] Cryopreserved sperm from Csp-12$^{-/-}$ mice were purchased from the Mutant Mouse Regional Resource Center (Chapel Hill, NC, USA) and injected into a surrogate wt female. The litter resuscitated from the cryoarchive was genotyped, and breeding was carried out by monogamous mating. A pair of male and female homozygous Csp-12$^{-/-}$ mice were kept in the same cage for mating. Pups were weaned at the age of 3 weeks and separated according to sex. Animals were maintained in a 12-hour light/dark cycle with unlimited access to food and water. The T17M genotyping was performed as previously described.[6] All studies were performed in accordance with the ARVO Statement for the Use of Animals in Ophthalmic and Vision Research.

Electroretinography

Mice were dark adapted overnight, then anesthetized with ketamine (100 mg/kg) and xylazine (10 mg/kg), followed by dilation of pupils in dim red light with 2.5% phenylephrine hydrochloride ophthalmic solution (Akorn, Inc., Lake Forest, IL, USA). Scotopic ERGs were recorded using a wire contacting the corneal surface with 2.5% hypromellose ophthalmic demulcent solution (Akorn, Inc.). Electroretinography was performed at different light intensities (0 dB [2.5 cd*s/m^2], 5 dB [7.91 cd*s/m^2], 10 dB [25 cd*s/m^2], and 15 dB [79.1 cd*s/m^2]). Five scans were performed and averaged at different light intensities. The a-wave amplitudes were measured from the baseline to the peak in the cornea-negative direction, and the b-wave amplitudes were determined from the cornea-negative peak to the major cornea-positive peak. The signal was amplified, digitized, and stored using the LKC UTAS-3000 Diagnostic System (Gaithersburg, MD, USA).

Spectral-Domain Optical Coherence Tomography

Spectral-domain optical coherence tomography (SD-OCT) was performed in 1-, 2-, and 3-month-old animals using the Spectral Domain Ophthalmic Imaging System (SDOIS; Bioptigen, Morrisville, NC, USA). The mice were anesthetized as described above. Horizontal volume scans through the area dorso-temporal to the optic nerve (superior retina) and the area ventro-temporal to the optic nerve (inferior retina) were used to evaluate the thickness of the outer nuclear layer (ONL). For measuring the thickness of the ONL, six calibrated calipers were placed in the superior and inferior hemispheres of retinas within 100, 200, 300, and 400 μm of the optic nerve head. The thickness of the ONL was determined by averaging 10 measurements.

Histology

For hematoxylin and eosin staining, mouse eyes were enucleated at 1 and 3 months of age and were fixed overnight in 4% freshly made paraformaldehyde in phosphate-buffered saline (PBS). Afterwards, eye cups were transferred to PBS to remove formaldehyde and submerged sequentially in solutions of 10%, 20%, and 30% sucrose for at least 1 hour each. Eye cups were then embedded in cryostat compound (Tissue TEK OCT; Sakura Finetek USA, Inc., Torrance, CA, USA) and frozen at −80°C. Also, 12-μm sections were obtained by using cryostat. Slides with right and left retinas were used for further histological analysis. To count the nuclei of photoreceptors, we stained cryostat sectioned retinas with hematoxylin and eosin. Digital images of right and left retinas of individual mice were analyzed in the central superior and inferior, equally located from the optic nerve head. Images were analyzed by a masked investigator.

Quantitative Real-Time RT–PCR

For RNA extraction, whole retinas were isolated from 1-month-old mice (wt, Csp-12$^{-/-}$, T17M, and T17M Csp-12$^{-/-}$) by surgical excision. Total RNA was extracted using the Qiagen RNeasy Mini Kit (Valencia, CA, USA). One microgram purified RNA was reverse transcribed into cDNA using iScript Reverse Transcription Supermix (Bio-Rad, Hercules, CA, USA). Integrity of the RNA samples and efficiency of the cDNA reaction were verified prior to the quantitative (q)RT-PCR. TaqMan Gene Expression Assay for *caspase-12* (ID: Mm00802897_m1) and *Bax* (ID: Mm00432051_m1) from Applied Biosystems (Carlsbad, CA, USA) was used to measure gene expression. Quantitative real-time PCR was performed with the Step One Plus Real-Time PCR System (Applied Biosystems) based on the relative standard curve method. Reactions were performed at 50°C for 2 minutes and 95°C for 10 minutes, followed by 40 cycles at 95°C for 15 seconds and 60°C for 1 minute. Results were expressed as cycle threshold time (Ct) and were

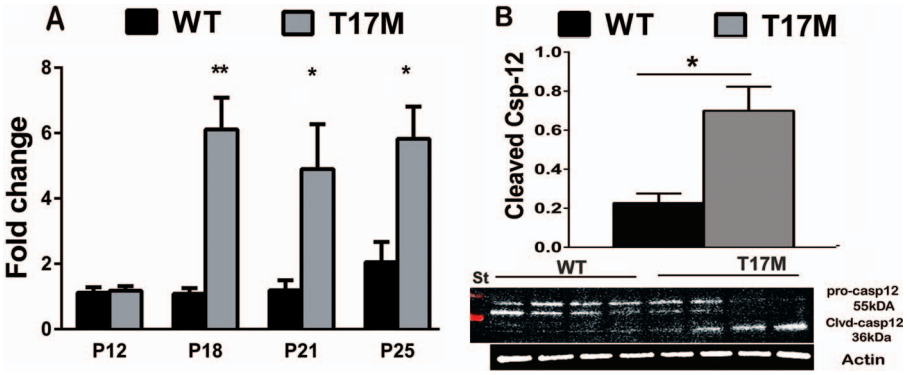

FIGURE 1. Expression and activation of Csp-12 in the T17M retina during ADRP progression. We used four animals per group in this experiment and analyzed retinal protein and RNA extracts at early time points from P12 to P25. (**A**) Starting at P18, we observed a 6-fold ($P < 0.01$) increase in *Csp-12* mRNA in T17M mice compared with wt. At P21 and P25, *Csp-12* gene expression was upregulated between 4.5- and 1.6-fold. (**B**) At P21, we detected a 3-fold ($P < 0.001$) increase in Csp-12 activation in T17M retinas, suggesting that in addition to the UPR activation detailed in previous studies,[4,6] ADRP photoreceptors also experience activation of Csp-12. One-way ANOVA was used to calculate differences. Data are shown as mean ± SEM (*$P < 0.05$, **$P < 0.01$).

normalized to Ct times for the housekeeping gene *Gapdh*. The replicated RQ (relative quantity) values for each biological sample were averaged. Four biological samples from each strain were used for qRT-PCR analyses.

Western Blot Analysis

For protein extraction, whole retinas were isolated from 1-month-old mice (wt, Csp-12$^{-/-}$, T17M, and T17M Csp-12$^{-/-}$) by surgical excision. Total protein was extracted via sonication in a protein extraction buffer containing 25 mM sucrose, 100 mM Tris-HCl, pH = 7.8, and a mixture of protease inhibitors (phenylmethylsulfonyl fluoride [PMSF], N-alpha-tosyl-L-lysinyl-chloromethylketone [TLCK], aprotinin, leupeptin, and pepstatin). Protein concentrations were determined using Bio-Rad Protein Assays based on the Bradford method of protein quantitation. Proteins (30–40 μg) were separated on 4% to 20% Criterion Precast gels (Bio-Rad), transferred to a polyvinylidene difluoride (PVDF) membrane using the Trans-Blot Turbo Transfer System (Bio-Rad), and incubated with primary antibodies (calpastatin 4146, BAX 2772, TRAF2 4712, and cleaved caspase-3 9664 from Cell Signaling [Danvers, MA, USA] and caspase-12 ab18766 from Abcam [Cambridge, MA, USA]) overnight at 4°C with agitation. Goat anti-rabbit (1:10,000, 926-68021) and donkey anti-mouse (1:10,000, 926-32210) secondary antibodies were used (LI-COR Odyssey, Lincoln, NE, USA). β-actin was used as a gel loading control and was detected using an anti-β-actin antibody (1:5000, A1978; Sigma-Aldrich Corp., St. Louis, MO, USA). The developed membrane was imaged using the LI-COR Odyssey Quantitative Fluorescence Imaging System.

Calpain Activation Assay

The detection of calpain activity was performed using the Calpain Activity Assay kit from BioVision (Milpitas, CA, USA) in accordance with the manufacturer's recommendations and compared the activation of calpains in wt, Csp-12$^{-/-}$, T17M, and T17M Csp-12$^{-/-}$ retinal tissues. Detection of the cleavage substrate Ac-LLY-AFC was performed in a fluorometer (PerkinElmer, Inc., Waltham, MA, USA) that was equipped with a 400-nm excitation filter and 505-nm emission filter.

Caspase-3/7 Activity Assay

The detection of Csp-3/7 activity was performed using the Caspase-Glo 3/7 Luciferase assay (G8091; Promega, Madison, WI, USA) kit in accordance with the manufacturer's recommendations. Luciferase signal was read by a luminescent plate reader (Infinite m200; PerkinElmer, Inc.) and used to compare the activation of Csp-3/7 in wt, Csp-12$^{-/-}$, T17M, and T17M Csp-12$^{-/-}$ retinal tissues.

Statistics

Two-way ANOVA comparisons were used to calculate differences in a- and b-wave ERG amplitudes and in the average ONL thickness of inferior and superior retinas in 1-, 2-, and 3-month-old mice. A one-way ANOVA and *t*-test were used to calculate fold change in mRNA expression and the level of normalized proteins in P30 retinas. For all experiments, a P value < 0.05 was considered significant (*$P < 0.05$, **$P < 0.01$, ***$P < 0.001$, ****$P < 0.0001$). Data are represented using mean ± SEM.

RESULTS

T17M mice experience UPR activation in their retinas starting at P15. Thus, being interested in the mechanism of photoreceptor cell death and ER stress–induced apoptosis, we analyzed *Csp-12* mRNA expression from P12 to P25.

T17M Mouse Retinas Demonstrate an Increase in the Expression and Activity of Csp-12

Figure 1 presents the results of qRT-PCR analysis demonstrating that *Csp-12* mRNA expression increased significantly in T17M retinas and was upregulated 6-fold at P18, prior to declining by 2-fold at P25. At P21 this increase resulted in a 3-fold elevation of cleaved Csp-12 protein, suggesting that ER stress–induced Csp-12 might play a pivotal role in activation of the apoptotic photoreceptor cell death shown in our earlier experiments.[2,4,6] Upregulation of Csp-12 activity during ADRP progression prompted us to try to determine a role for Csp-12 in retinal pathogenesis of T17M mice.

Csp-12 Ablation Significantly Delays Loss of Function for T17M Photoreceptors

We crossed T17M mice with Csp-12$^{-/-}$ mice and followed them by functional and histological analysis, as well as by SD-OCT, over a period of 3 months. Figure 2 presents the results of the scotopic ERG analysis of 1-, 2-, and 3-month-old T17M Csp-12$^{-/-}$ mice. The data demonstrated that the range of

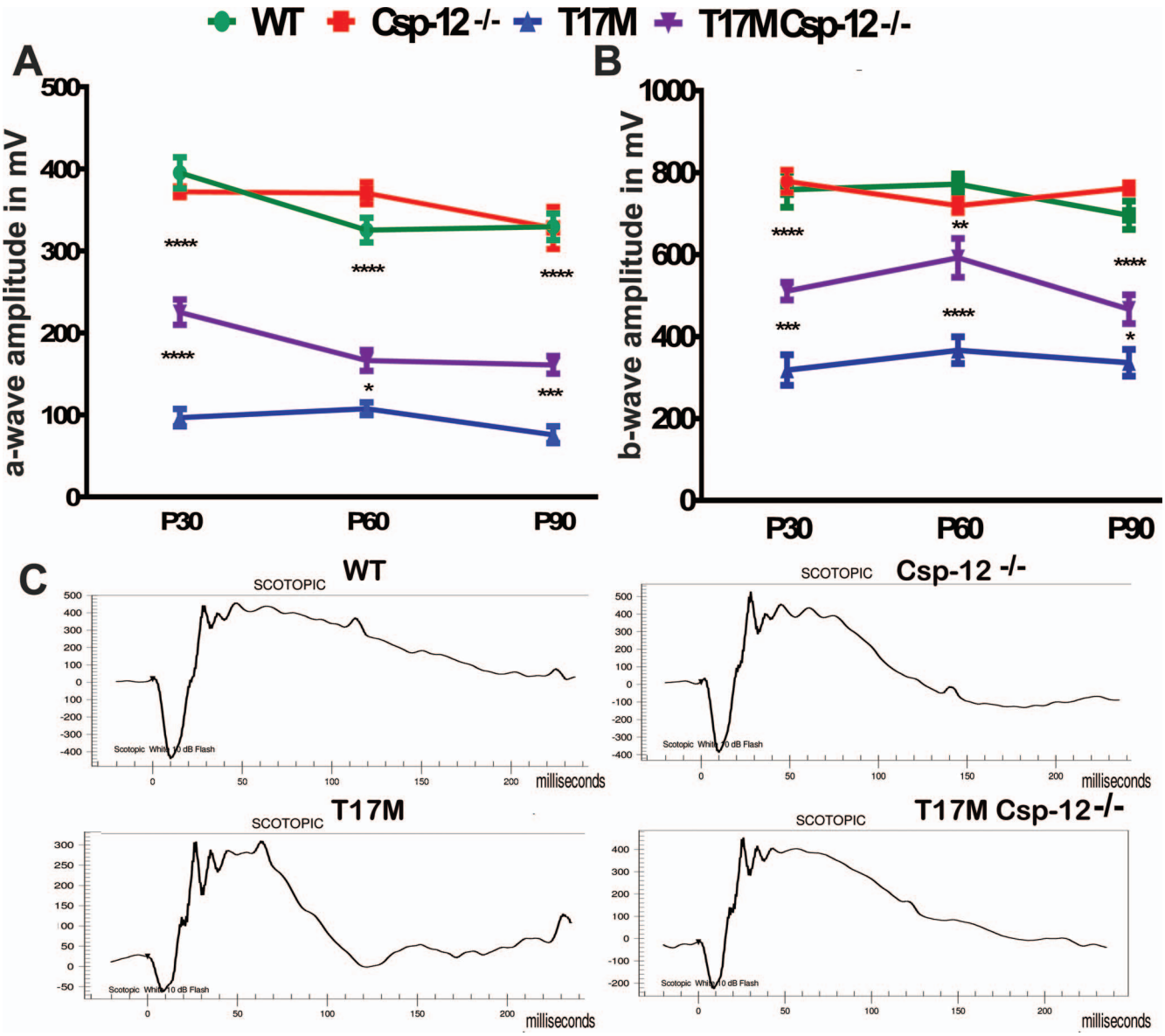

Figure 2. Lack of Csp-12 protects T17M retinas from degeneration, as measured by scotopic ERG responses at 10 dB. We analyzed four groups of animals ($n = 6$). (**A**) Using two-way ANOVA, we demonstrated that a-wave amplitudes of the scotopic ERG were significantly increased in T17M Csp-12$^{-/-}$ mice at 1 month of age and that the value of a-wave amplitudes was 225 μV ± 15 vs. 97.0 μV ± 11 in T17M. These data represent a 2.3-fold difference in a-wave amplitudes between T17M and T17M Csp-12$^{-/-}$ mice. At 2 and 3 months, the difference between T17M and T17M Csp-12$^{-/-}$ groups was also dramatic, but somewhat diminished due to a decrease in T17M Csp-12$^{-/-}$ a-wave amplitudes. For example, we registered 166.0 μV ± 13 vs. 108.0 μV ± 7.8 and 161.0 μV ± 11 vs. 76.0 μV ± 10.0 in T17M Csp-12$^{-/-}$ versus T17M at 2 and 3 months, respectively. (**B**) Interestingly, b-wave scotopic ERG amplitudes were also elevated in T17M Csp-12$^{-/-}$ retinas. However, the magnitude of this elevation was less dramatic than for a-wave over the 3 examined months. Thus, 1-month-old T17M Csp-12$^{-/-}$ mice demonstrated 511.0 μV ± 22.0 vs. 318.0 μV ± 37.0 in T17M. In the second month, the b-wave amplitudes in the T17M Csp-12$^{-/-}$ mice were also increased by 1.6-fold as compared to T17M. We registered the b-wave amplitude of 592.2 μV ± 22.0 in T17M Csp-12 vs. 366.8 μV ± 32.0 in T17M. By 3 months of age the stable preservation of b-wave amplitude observed during the first 2 months changed, and the ratio of T17M Csp-12 to T17M amplitudes dropped from 1.6- to 1.38-fold (Supplementary Table S1). This would suggest that the bipolar cells are less sensitive to Csp-12 ablation in degenerating retinas. The differences between all groups were statistically significant. (**C**) Images of the scotopic ERG amplitudes registered at 10 dB or 25 cd*s/m^2 in four groups of animals. Data are shown as mean ± SEM (*$P < 0.05$, **$P < 0.01$, ***$P < 0.001$, ****$P < 0.0001$).

photoreceptor-specific a-wave amplitude in 1-, 2-, and 3-month-old T17M Csp-12$^{-/-}$ mice increased from 2.3- to 2.1-fold, respectively, as compared with T17M mice. The b-wave amplitude of the scotopic ERG was also elevated in these animals. The degree of elevation was, however, less profound as compared to a-wave, thus suggesting that the photoreceptors expressing the aberrant rhodopsin and experiencing UPR activation were also the retinal cell type most responsive to removal of the UPR downstream player.

Csp-12 Ablation Significantly Delays Death of T17M Photoreceptors and Preserves Retinal Integrity

Figures 3A through 3C demonstrate that Csp-12 ablation prevents the loss of retinal integrity in the superior and inferior hemispheres of T17M retinas. The inferior retina demonstrated an increased preservation of the ONL thickness in response to Csp-12 ablation. In 1-, 2-, and 3-month-old T17M Csp-12$^{-/-}$ mice, we observed a 1.3-, 1.6-, and 1.8-fold increase

in the ONL thickness as compared to T17M mice. Similarly, in the superior retina the average thickness of the ONL measured in 1-, 2-, and 3-month-old T17M Csp-12$^{-/-}$ mice by SD-OCT was increased from 1.2- to 1.5-fold, respectively. We next wanted to compare the data obtained by SD-OCT analysis with results from histological analysis and counted rows of photoreceptor nuclei using images of cryostat-sectioned retinas stained with H&E (Figs. 3D, 3E). The data revealed that in 1-month-old T17M Csp-12$^{-/-}$ mice, the prevention of photoreceptor cell death was more noticeable and reached 10 rows versus the 6.7 rows measured in T17M retinas. However, by 3 months of age we observed a further decline in the number of photoreceptor rows in T17M Csp-12$^{-/-}$ retinas, with an average of 7.9 rows. This would suggest that Csp-12 ablation does not arrest photoreceptor cells death but instead delays it.

Next, looking for the molecular mechanisms responsible for the above-mentioned delay and knowing that two independent pathways may activate Csp-12, we looked for biomarkers of Ca^{2+}-induced cell death and IRE1-TRAF2 activation.

Csp-12 Ablation in T17M Retinas Significantly Modifies Expression of Ca^{2+} Sensor Genes and Reduces Apoptosis

It has been proposed that in the case of retinal degeneration caused by expression of aberrant rhodopsin, an imbalance in Ca^{2+} homeostasis and elevation of intracellular Ca^{2+} may provoke cellular signaling leading to photoreceptor cell death.[18–21] Indeed, an increase in the levels of intracellular Ca^{2+}, regardless of whether this is a physiological or pathological event, activates a number of enzymes directly, or indirectly via Ca^{2+}-binding proteins. We analyzed the activity of μ-calpain and m-calpain in P30 T17M Csp-12$^{-/-}$ retinas (Fig. 4) since they are the major calpain forms expressed in retinas and because of their well-documented pathological roles in necrotic photoreceptor cell death.[21] Results from this experiment revealed that while the total μ- and m-calpain activity in T17M retinas increased by 3-fold as compared to wt, T17M Csp-12$^{-/-}$ retinas demonstrated a 2-fold decrease in the level of total calpain activity as compared to T17M retinas. This decrease was not statistically different when compared to wt. Thus, these results indicated that ablation of Csp-12 significantly downregulates calpain activity in degenerating retinas.

Calpastatin (calcium-dependent cysteine protease) is an endogenous calpain inhibitor protein consisting of an N-terminal domain L and four repetitive calpain inhibition domains (domains 1–4).[22] We analyzed its levels in degenerating retinas and found it to be elevated 4.5-fold in T17M Csp-12$^{-/-}$ retinas versus T17M, reaching levels found in wt retinas. These data were in agreement with data from a calpain activity assay and indicated calpain inhibition in T17M degenerating retinas by calpastatin as a therapeutic approach leading to retardation of retinal degeneration.

In our previous studies,[2,23] we demonstrated increased BAX (Bcl-2-associated X protein) expression and its translocation to the mitochondria. Bcl-2-associated X protein is known to be involved in ER Ca^{2+}-mediated apoptosis and to antagonize the ER Ca^{2+}-modulating activities of Bcl-2 and Bcl-XL.[24] Therefore, in the current study we also analyzed BAX expression.

We found that levels of *Bax* mRNA were elevated in both ADRP (T17M and T17M Csp-12$^{-/-}$) groups as compared to Csp-12$^{-/-}$ mice and did not differ from levels in wt retinas (Fig. 4C). However, we detected a 24-fold increase in BAX protein in T17M retina when compared to wt mice. Ablation of Csp-12 in these retinas downregulated BAX levels significantly by 3.8-fold. However, despite the significant decline in BAX protein in T17M Csp-12$^{-/-}$ mice, its level was still over 6-fold upregulated when compared to wt retinas (Figs. 4D, 4E). These results suggested that despite similar *Bax* mRNA expression levels in the two ADRP groups, there were differences either in the translation efficiency or in the degradation of BAX. It is also possible that the examined retinas had different levels of BAX inhibitor protein 1, which is known not only to downregulate BAX protein but to also control the IRE 1-TRAF2 pathway.[25]

Keeping this in mind, we then analyzed the level of TRAF2 protein and Csp-3/7 activity in degenerating retinas (Figs. 5A–C). As in our previous study of T17M mice with activated IRE1-TRAF2-cJun signaling,[6] we found in the current study that TRAF2 protein was significantly elevated in T17M ADRP retinas. Interestingly, Csp-12 ablation in T17M retinas significantly diminished TRAF2 levels, suggesting that the proapoptotic IRE1-TRAF2-cJUN pathway was also downregulated in these retinas.

We next found that the decrease in TRAF2 protein was associated with a 2-fold decline in total Csp-3/7 activity in T17M Csp-12$^{-/-}$ mice as compared to T17M animals. The latter animals demonstrated significant upregulation of Csp-3/7 activity as compared to wt, supporting a previously proposed hypothesis for the involvement of apoptosis in the mechanism of photoreceptor cell death[26,27] in addition to nonapoptotic pathways.[21] We found that the level of active Csp-3/7 in T17M Csp-12$^{-/-}$ retinas was not statistically different from that found in wt and Csp-12$^{-/-}$ retinas using one-way ANOVA. However, a *t*-test demonstrated a 50% increase in cleaved Csp-3/7 in T17M Csp-12$^{-/-}$ retinas as compared to wt ($P = 0.026$). To verify difference between T17M Csp-12 and wt retinas as seen by the activity assay, we also performed Western blots, which demonstrated that the activation of Csp-3 in T17M Csp-12 retinas was 42% lower than in T17M retinas and 990% higher than in wt retinas. This experiment suggested that Csp-mediated signaling is still active in T17M Csp-12 retinas. Therefore, we next attempted to answer the question whether any additional prodeath pathways are activated in T17M Csp-12 retinas that would inhibit cell defense signaling.

Out of the list of potential prodeath cellular signaling pathways, we decided to examine the regulation of nuclear factor (NF)-κB activity. Nuclear factor-κB is known to control the inflammatory response in cells, and together with TNFa, monocyte chemoattractant protein (MCP)-1, and IL-6 was found to be upregulated in P15 T17M retinas.[3] To determine if Csp-12 ablation in P30 T17M retinas elevates NF-κB signaling in response to, as an example, microbial infection and thus causes photoreceptor cell death, we analyzed the levels of NF-κB (p65). We were interested in NF-κB in particular because NF-κB-promoted signaling has been shown to be activated in the Csp-12$^{-/-}$ mouse experimental model of colonic inflammation.[28] We thus excluded the possibility of enhancing photoreceptor cell death via an enhanced NF-κB-mediated inflammatory response and demonstrated that Csp-12 ablation slightly reduced p65 NF-κB activity in T17M Csp-12 retinas as compared to T17M retinas ($P = 0.009$). Given that NF-κB levels were still higher than in wt retinas, this suggests that NF-κB activation was due to expression of T17M RHO in the retinas.

Discussion

Previously, we have reported that the rate of retinal degeneration in ADRP animals could be modified by knockdown or overexpression of UPR mediators.[4,6,29] In T17M RHO mice we have demonstrated that Csp-7 ablation significantly slowed the onset of retinal degeneration. As a logical continuation of that study, we did the work presented here, in which we revealed that ablation of ER stress–associated Csp-12 also partially blocks deterioration of T17M RHO retinas. However, despite

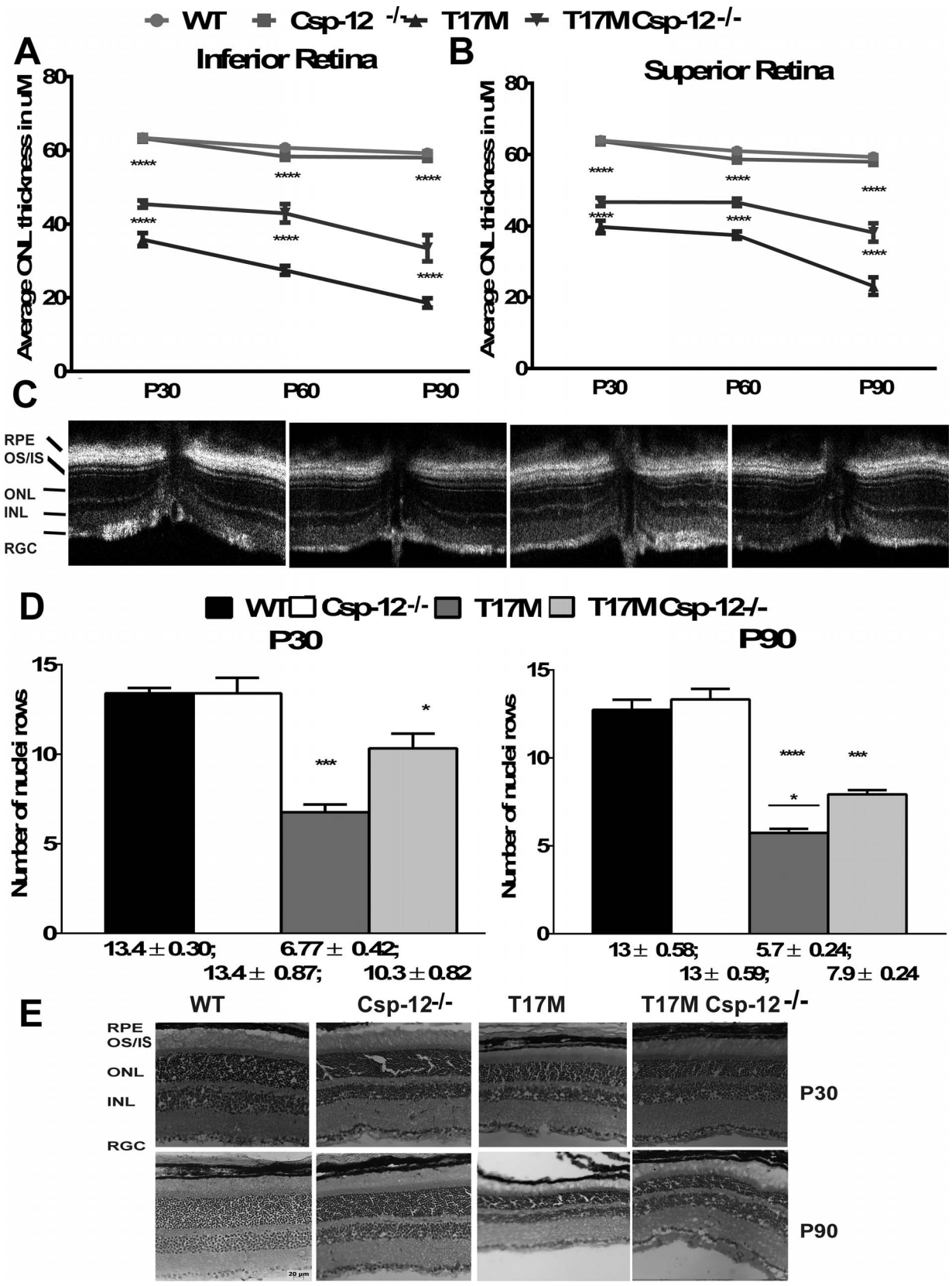

Figure 3. The preservation of retinal structure and prevention of photoreceptor cell death in T17M Csp-12$^{-/-}$ retinas. We analyzed four groups of animals ($n = 6$). (**A**) Two-way ANOVA analysis of data from the inferior retina revealed that this region was better preserved than the superior region, with increases in the average ONL thicknesses over a period of 3 months of 1.26-, 1.56-, and 1.8-fold. These data also pointed to the fact that despite experiencing the same molecular mechanisms responsible for retinal denegation, activation of prodeath cascades in the inferior and superior regions might occur to different degrees, suggesting that the therapeutic benefit from Csp-12 ablation could also be different. (**B**) Interestingly, the data demonstrated a steady preservation of the average ONL thickness in T17M Csp-12$^{-/-}$ superior retinas from 1.2 to 1.5 over a period of 3 months,

while T17M mice experienced a continuous decline in the average ONL thickness. (**C**) Spectral-domain OCT representative images of wt, Csp-12$^{-/-}$, T17M, and T17M Csp-12$^{-/-}$ retinas. (**D**) Histological analyses of wt, Csp-12$^{-/-}$, T17M, and T17M Csp-12$^{-/-}$ cryostat-sectioned retinas stained with hematoxylin and eosin (H&E). Results from photoreceptor row counts in control and experimental mouse retinas at 1 and 3 months of age show preservation of photoreceptor cell death in T17M Csp-12$^{-/-}$ mice. Results from histological analysis of H&E-stained cryostat sections demonstrated partial preservation of T17M retinas from photoreceptor cell death. For example, 1-month-old T17M Csp-12$^{-/-}$ had 10.3 ± 0.82 rows, and this number was significantly (1.5-fold) higher when compared to T17M retinas (6.7 ± 0.82). However, by 3 months of age, the number of photoreceptor rows in T17M Csp-12$^{-/-}$ had already declined to 7.9 ± 0.24 rows, and preservation was only 1.38 times higher as compared to T17M mice (5.7 ± 0.24). Two-way ANOVA with multiple comparison analysis demonstrated differences in all three groups of animals at 1 and 3 months of age. (**E**) Representative images of 1- and 3-month-old wt, Csp-12, T17M, and T17M Csp-12$^{-/-}$ retinas stained with H&E. RGC, retinal ganglion cell layer; INL, inner nuclear layer; ONL, outer nuclear layer; IS, inner segments; OS, outer segments. *Scale bar*: 20 μm. Data are shown as mean ± SEM (*$P < 0.05$, ***$P < 0.001$, ****$P < 0.0001$).

this partial cytoprotective effect, the physiological response and alleviation of photoreceptor cell loss are more striking in animals deficient in Csp-7 than in Csp-12. This observation would confirm that Csp-12 is upstream of the executive Csp-7 and that Csp-7 might activate alternate signaling such as cleavage of automodified poly (ADP-ribose) polymerase[30] resulting in cell death in T17M retinas. Nevertheless, even though deficiencies in both caspases significantly retard retinal degeneration, our results suggested that blocking apoptotic signaling alone in ADRP photoreceptors is not sufficient to prevent vision loss and the gradual loss of ADRP photoreceptors.

We found that scotopic ERG a- and b-wave amplitudes are preserved in T17M Csp-12$^{-/-}$ mice, and these results are in agreement with the delay of onset of photoreceptor cell death in these animals. However, ratios of a- and b-wave amplitudes registered in either T17M Csp-7$^{-/-}$ or T17M Csp-12$^{-/-}$ to corresponding amplitudes in T17M mice are higher in the first group of animals, suggesting a stronger preservation of ADRP photoreceptors. This was also the case when comparing SD-OCT results and photoreceptor row counts in H&E-stained cryostat sections from both groups. The results demonstrate that higher preservation of a physiological response corresponds to a more prominent protection and viability of photoreceptor cells.

Ablation of Csp-12 significantly dampened Ca^{2+}-promoted calpain activation and dramatically enhanced a cellular defense mechanism activated by increased calpastatin expression. These data also point to calpastatin as a potential therapeutic target that was capable of exerting a cytoprotective effect by countering Ca^{2+}-induced calpain activation. The data indirectly imply that there could be a decreased

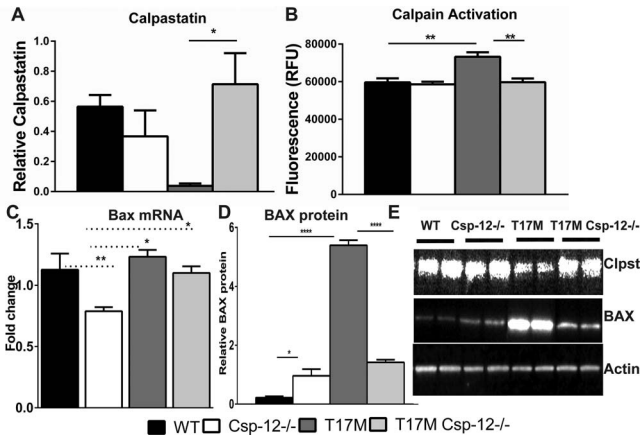

Figure 4. Ca^{2+} sensor protein expression in T17M Csp-12$^{-/-}$ retinas. Western blot analysis of retinal protein extracts isolated from four animals in each group at P30. Statistical analysis was performed by using one-way ANOVA. (**A**) We found that the total calpain activity was increased in T17M retinas by 1.25-fold as compared to wt. Csp-12 ablation, however, dramatically decreased the levels of active calpains in these retinas and reduced them to wt levels. (**B**) In agreement with downregulation of calpain activity in T17M Csp-12$^{-/-}$ mice, we found that the calpain inhibitor calpastatin was upregulated by 4.5-fold in ADRP retinas that were deficient in the ER stress–associated Csp-12. This points to a link between calpain activation and the calpain inhibitor. Both of these results were in agreement with downregulation of BAX in T17M Csp-12$^{-/-}$ retinas. Although the *Bax* mRNA levels in the two ADRP groups were not significantly different (**C**), BAX protein production was significantly elevated in T17M retinas and was dramatically decreased (3.8-fold) in T17M Csp-12 mice (**D**), suggesting less inhibition of the antiapoptotic BCL-2 protein and, consequently, stronger antiapoptotic activity undermining ADRP progression in T17M Csp-12$^{-/-}$ retinas. (**E**) Representative images of Western blots treated with calpastatin-, BAX-, and actin-specific antibodies. Data are shown as mean ± SEM (*$P < 0.05$, **$P < 0.01$, ****$P < 0.0001$).

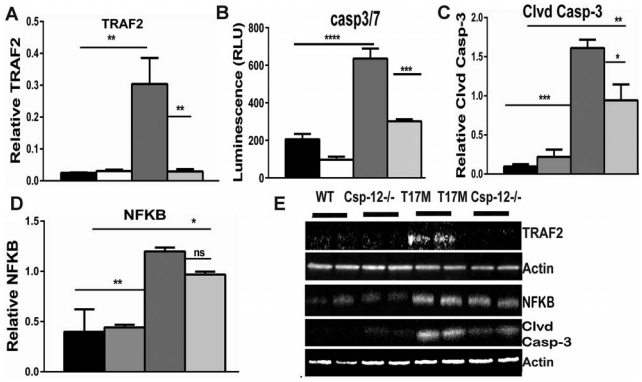

Figure 5. Csp-12 ablation in T17M retinas results in decreased levels of apoptosis. Four animals in each group were analyzed using one-way ANOVA. (**A**) In the current study we confirmed that the level of TRAF2 was 12-fold higher in T17M retinas, implying that the apoptotic IRE1-TRAF2-cJNK pathway could be upregulated in these retinas. Ablation of Csp-12, however, dramatically cut TRAF2 protein expression to levels comparable to wt. (**B**) Interestingly, downregulation of TRAF2 in T17M Csp-12$^{-/-}$ retinas occurred concomitantly with a decline in Csp-3/7 activity in T17M Csp-12$^{-/-}$ retinas. However, the level of active caspases was still 50% higher as compared to that in wt retinas. (**C**) Reduction of Csp-3 was confirmed by Western blot analysis. Csp-3 activation was found to be 16.9-fold higher in T17M retinas than in wt retinas. Meantime, ablation of Csp-12 in ADRP retinas led to diminished Csp-3 activity. The observed increase in Csp-3 activity in T17M Csp-12 retinas reached 9.9-fold as compared to wt retinas. These results, along with the observed TRAF2 downregulation, indicate that a reduction in apoptotic signaling in ADRP retinas resulted in partial protection of photoreceptors from functional loss and cell death. (**D**) NF-κB activity (p65) was measured in all four groups of animals. A greater than 3-fold elevation was found in T17M retinas as compared to wt retinas. A slight decline in NF-κB expression was observed in T17M Csp-12 mice as compared to T17M retinas, which was not statistically different when compared by one-way ANOVA but was significant when compared by *t*-test ($P = 0.009$). Despite its 20% downregulation, the level of NF-κB in T17M Csp-12 mice was still 2.4-fold higher than in wt retinas. (**E**) Representative images of Western blots treated with TRAF2-, NF-κB, Csp-3, and actin-specific (internal control) antibodies. Data are shown as mean ± SEM (*$P < 0.05$, **$P < 0.01$, ***$P < 0.001$, ****$P < 0.0001$).

concentration of free cytosolic Ca^{2+} in T17M Csp-12$^{-/-}$ retinas. In support of this hypothesis, we observed a dramatic reduction of BAX protein, which is known to regulate calcium efflux from the ER, thus potentially influencing Ca^{2+}-mediated apoptosis.[31]

Both Csp-7 and Csp-12 ablation in T17M retinas result in reduction of TRAF2 protein. In our previous study we hypothesized that reduction of Csp-12 may affect TRAF2 protein expression in T17M mice.[6] In the current study we provide evidence supporting the fact that there is a feedback loop between TRAF2 and Csp-12 proteins in the retina. Interestingly, both the ER stress-IRE1-TRAF2-Csp12-Csp3/7 and the calcium-induced active calpain-Csp-12-Csp-3/7 pathways contribute to retinal pathogenesis in T17M mice through activation of Csp-12. However, in both cases the inhibition of Csp-12 leads to partial preservation of ADRP photoreceptors.

Interestingly, the neuroprotective effect of Csp-12 ablation is not outweighed by enhancement of NF-κB-mediated inflammatory signaling at P30, which otherwise would result in enhanced photoreceptor cell death at later stages of ADRP. This suggests that, in addition to the Csp-12–regulated TRAF6-Rip2–NF-κB inflammatory response, T17M retinas might have alternate Rip kinases (Rip1), which promote TRAF6-mediated signaling. Alternatively, T17M retinas might experience the triggering of other noncanonical NF-κB activation pathways such as CK2-calpain.[32] Indeed, lack of NF-κB level alteration in T17M Csp-12 retinas suggests that this signaling is not controlled by Csp-12 in P30 retinas. T17M retinas expressing Csp-12 already demonstrate activation of the NF-κB–inflammatory response at P15[3] that perhaps contributes tremendously to photoreceptor cell death. However, this signaling is associated with expression of aberrant mutant RHO. Ablation of Csp-12 does not promote a stronger NF-κB-mediated downstream pathway than typically found in T17M retinas, and this fact suggests that enhanced photoreceptor cell death in T17M Csp-12 retinas due to overexpression of NF-κB is unlikely. However, these data also point to NF-κB as a target for manipulating the inflammatory response in order to delay the onset of retinal degeneration in T17M retinas.

Nevertheless, together with results obtained in T17M mice deficient in Csp-7, we have demonstrated that reducing the level of apoptosis alone by Csp-12 ablation is not sufficient to rescue ADRP photoreceptors.

That said, we have validated Csp-12 as a potential therapeutic target, which in combination with nonapoptotic molecular targets might be efficiently used to arrest retinal degeneration in ADRP patients.

Acknowledgments

Supported by National Institutes of Health Grant R01EY020905.

Disclosure: **Y. Bhootada**, None; **S. Choudhury**, None; **C. Gully**, None; **M. Gorbatyuk**, None

References

1. Li T, Sandberg MA, Pawlyk BS, et al. Effect of vitamin A supplementation on rhodopsin mutants threonine-17 → methionine and proline-347 → serine in transgenic mice and in cell cultures. *Proc Natl Acad Sci U S A*. 1998;95:11933–11938.
2. Kunte MM, Choudhury S, Manheim JF, et al. ER stress is involved in T17M rhodopsin-induced retinal degeneration. *Invest Ophthalmol Vis Sci*. 2012;53:3792–3800.
3. Rana T, Shinde VM, Starr CR, et al. An activated unfolded protein response promotes retinal degeneration and triggers an inflammatory response in the mouse retina. *Cell Death Dis*. 2014;5:e1578.
4. Nashine S, Bhootada Y, Lewin AS, Gorbatyuk M. Ablation of C/EBP homologous protein does not protect T17M RHO mice from retinal degeneration. *PLoS One*. 2013;8:e63205.
5. Choudhury S, Nashine S, Bhootada Y, et al. Modulation of the rate of retinal degeneration in T17M RHO mice by reprogramming the unfolded protein response. *Adv Exp Med Biol*. 2014;801:455–462.
6. Choudhury S, Bhootada Y, Gorbatyuk O, Gorbatyuk M. Caspase-7 ablation modulates UPR, reprograms TRAF2-JNK apoptosis and protects T17M rhodopsin mice from severe retinal degeneration. *Cell Death Dis*. 2013;4:e528.
7. Viana RJ, Nunes AF, Rodrigues CM. Endoplasmic reticulum enrollment in Alzheimer's disease. *Mol Neurobiol*. 2012;46:522–534.
8. Gupta S, Cuffe L, Szegezdi E, et al. Mechanisms of ER stress-mediated mitochondrial membrane permeabilization. *Int J Cell Biol*. 2010;2010:170215.
9. Nakagawa T, Zhu H, Morishima N, et al. Caspase-12 mediates endoplasmic-reticulum-specific apoptosis and cytotoxicity by amyloid-beta. *Nature*. 2000;403:98–103.
10. Yoneda T, Imaizumi K, Oono K, et al. Activation of caspase-12, an endoplastic reticulum (ER) resident caspase, through tumor necrosis factor receptor-associated factor 2-dependent mechanism in response to the ER stress. *J Biol Chem*. 2001;276:13935–13940.
11. Sergeev IN. Calcium signaling in cancer and vitamin D. *J Steroid Biochem Mol Biol*. 2005;97:145–151.
12. Marsili S, Genini S, Sudharsan R, Gingrich J, Aguirre GD, Beltran WA. Exclusion of the unfolded protein response in light-induced retinal degeneration in the canine T4R RHO model of autosomal dominant retinitis pigmentosa. *PLoS One*. 2015;10:e0115723.
13. Mockel A, Obringer C, Hakvoort TB, et al. Pharmacological modulation of the retinal unfolded protein response in Bardet-Biedl syndrome reduces apoptosis and preserves light detection ability. *J Biol Chem*. 2012;287:37483–37494.
14. Mohlin C, Taylor L, Ghosh F, Johansson K. Autophagy and ER-stress contribute to photoreceptor degeneration in cultured adult porcine retina. *Brain Res*. 2014;1585:167–183.
15. Thapa A, Morris L, Xu J, et al. Endoplasmic reticulum stress-associated cone photoreceptor degeneration in cyclic nucleotide-gated channel deficiency. *J Biol Chem*. 2012;287:18018–18029.
16. Chen C, Cano M, Wang JJ, et al. Role of unfolded protein response dysregulation in oxidative injury of retinal pigment epithelial cells. *Antioxid Redox Signal*. 2014;20:2091–2106.
17. Saleh M, Mathison JC, Wolinski MK, et al. Enhanced bacterial clearance and sepsis resistance in caspase-12-deficient mice. *Nature*. 2006;440:1064–1068.
18. Shinde VM, Sizova OS, Lin JH, LaVail MM, Gorbatyuk MS. ER stress in retinal degeneration in S334ter Rho rats. *PLoS One*. 2012;7:e33266.
19. Ozaki T, Ishiguro S, Hirano S, et al. Inhibitory peptide of mitochondrial mu-calpain protects against photoreceptor degeneration in rhodopsin transgenic S334ter and P23H rats. *PLoS One*. 2013;8:e71650.
20. Kaur J, Mencl S, Sahaboglu A, et al. Calpain and PARP activation during photoreceptor cell death in P23H and S334ter rhodopsin mutant rats. *PLoS One*. 2011;6:e22181.
21. Arango-Gonzalez B, Trifunovic D, Sahaboglu A, et al. Identification of a common non-apoptotic cell death mechanism in hereditary retinal degeneration. *PLoS One*. 2014;9:e112142.
22. Sato K, Minegishi S, Takano J, et al. Calpastatin, an endogenous calpain-inhibitor protein, regulates the cleavage of the Cdk5 activator p35 to p25. *J Neurochem*. 2011;117:504–515.

23. Sizova OS, Shinde VM, Lenox AR, Gorbatyuk MS. Modulation of cellular signaling pathways in P23H rhodopsin photoreceptors. *Cell Signal*. 2014;26:665–672.
24. Sano R, Reed JC. ER stress-induced cell death mechanisms. *Biochim Biophys Acta*. 2013;1833:3460–3470.
25. Castillo K, Rojas-Rivera D, Lisbona F, et al. BAX inhibitor-1 regulates autophagy by controlling the IRE1 alpha branch of the unfolded protein response. *EMBO J*. 2011;30:4465–4478.
26. Chang GQ, Hao Y, Wong F. Apoptosis: final common pathway of photoreceptor death in rd, rds, and rhodopsin mutant mice. *Neuron*. 1993;11:595–605.
27. Marigo V. Programmed cell death in retinal degeneration: targeting apoptosis in photoreceptors as potential therapy for retinal degeneration. *Cell Cycle*. 2007;6:652–655.
28. LeBlanc PM, Yeretssian G, Rutherford N, et al. Caspase-12 modulates NOD signaling and regulates antimicrobial peptide production and mucosal immunity. *Cell Host Microbe*. 2008;3:146–157.
29. Gorbatyuk MS, Knox T, LaVail MM, et al. Restoration of visual function in P23H rhodopsin transgenic rats by gene delivery of BiP/Grp78. *Proc Natl Acad Sci U S A*. 2010;107:5961–5966.
30. Oliver FJ, de la Rubia G, Rolli V, Ruiz-Ruiz MC, de Murcia G, Murcia JM. Importance of poly(ADP-ribose) polymerase and its cleavage in apoptosis. Lesson from an uncleavable mutant. *J Biol Chem*. 1998;273:33533–33539.
31. Scorrano L, Oakes SA, Opferman JT, et al. BAX and BAK regulation of endoplasmic reticulum Ca2+: a control point for apoptosis. *Science*. 2003;300:135–139.
32. Godwin P, Baird AM, Heavey S, Barr MP, O'Byrne KJ, Gately K. Targeting nuclear factor-kappa B to overcome resistance to chemotherapy. *Front Oncol*. 2013;3:120.

Investigative Ophthalmology & Visual Science